# New tests of the gauge-fixing approach to lattice chiral gauge theories

Wolfgang Bock[a*], Maarten F.L. Golterman[b], Ka Chun Leung[a*] and Yigal Shamir[c]

[a]Institute of Theoretical Physics, University of Siegen, 57068 Siegen, Germany

[b]Department of Physics, Washington University, St. Louis, MO 63130, USA

[c]School of Physics and Astronomy, Beverly and Raymond Sackler Faculty of Exact Sciences, Tel-Aviv University, Ramat Aviv 69978, Israel



We report on recent progress with the gauge-fixing approach to lattice chiral gauge theories. The bosonic sector of the gauge-fixing approach is studied with fully dynamical U(1) gauge fields. We demonstrate that it is important to formulate the Lorentz gauge-fixing action such that the dense set of lattice Gribov copies is removed, and the gauge-fixing action has a unique absolute minimum. We then show that the spectrum in the continuum limit contains only the desired massless photon, as expected.

## 1. INTRODUCTION

A tractable non-perturbative formulation of chiral gauge theories with non-abelian gauge groups on the lattice is still an outstanding problem. However, some important progress was made recently for the abelian case.

The fermion formulations employed in most approaches break chiral gauge invariance. This implies that the fermions couple on the lattice to the longitudinal gauge degrees of freedom, a coupling that tends to render the theory vector-like in the continuum limit. This failure is related to the fact that the longitudinal gauge degrees of freedom are subject to strong fluctuations in symmetric phases which, in most cases, are the only places in the phase diagrams where a continuum limit with unbroken chiral symmetry can be defined (for a review see ref. [1]).

Progress was made recently when it was shown that, with a Dirac operator satisfying the Ginsparg–Wilson relation, it is possible to formulate chiral gauge theories without breaking gauge invariance or violating locality [2]. The above mentioned problems with the violation of gauge invariance do therefore, in principle, not apply in that case. In this formulation, the fermion measure includes a gauge-field dependent phase factor. This phase factor can be chosen such that the theory is gauge invariant and local, but an explicit expression for this phase factor was not given, and the approach is therefore, at least at this stage, not ready for numerical investigation. It is also not clear what the effects will be of the various approximations that will need to be made in order to implement this construction numerically, since these approximations will again break gauge invariance. Steps to generalize this approach to the non-abelian case can be found in ref. [3].

Here, instead, we focus on the gauge-fixing approach for the case of an abelian gauge group. The central idea is to transcribe the Lorentz gauge-fixed continuum theory to the lattice [4]. This approach allows one to use any of the standard lattice fermion formulations (which break chiral gauge invariance), like the chiral Wilson action [5–10] or domain-wall fermions [11]. Gauge invariance is restored in the continuum limit by adding a finite number of counterterms to the action. The abelian case is simpler in that the ghost part of the continuum action is free and, hence, can be omitted on the lattice.

A concrete lattice formulation of the gauge-fixing approach for an abelian theory with a non-linear gauge-fixing condition was first given in

*presenters at conference

ref. [5]. Later a formulation was also given for the Lorentz gauge [6]. The central question is whether the longitudinal degrees of freedom are sufficiently "tamed" by the gauge-fixing action, such that their interactions with the fermions become irrelevant. We have addressed this issue in a series of publications [7–9] in a reduced limit where the transversal degrees of freedom are left out, and only the dynamics of the longitudinal degrees of freedom is taken into account. That model has a continuum limit corresponding to a second order phase transition between a ferromagnetic (FM) and a so-called ferromagnetic directional (FMD) phase (see below). Both FM and FMD are *not* symmetric phases, and therefore the no-go arguments of ref. [12] do not apply. We showed that all symmetries of the target continuum theory are restored at the FM-FMD phase transition [7,8]. In particular, the fermion spectrum contains only the desired chiral states [8,9].

What was missing is a study of the gauge-fixing approach with a fully dynamical U(1) gauge field. This study is carried out here, with attention restricted to the purely bosonic sector of the theory. The reason is that, once the existence of the correct (bosonic and fermionic) massless spectrum is established in the continuum limit, the validity of perturbation theory assures that the correct chiral gauge theory will emerge when the coupling between the full gauge and fermion fields is restored.

Two topics will be addressed in this contribution. 1.) The Lorentz gauge-fixing action can be discretized in different ways. We will give strong evidence that, in order to obtain the desired continuum limit, the gauge-fixing action should have a unique classical vacuum. 2.) It will be demonstrated that only the correct state, namely a (free) massless photon, is reproduced in the continuum limit of the purely bosonic sector.

## 2. LATTICE FORMULATION

The purely bosonic U(1) lattice theory is defined by the following path integral

$$Z = \int DU \, \exp(-S(U)) \tag{1}$$

$$= \int DU D\phi \, \exp(-S(\phi_x^\dagger U_{\mu x} \phi_{x+\hat{\mu}})) \, , \tag{2}$$

$$S = S_{\rm G}(U) + S_{\rm g.f.}(U) + S_{\rm c.t.}(U) \, , \tag{3}$$

where in eq. (2) we made the integration over the longitudinal degrees of freedom explicit through a group-valued Higgs-Stückelberg field $\phi_x$. The action includes three terms: the standard plaquette action $S_{\rm G}(U) = \frac{1}{g^2} \sum_{x\mu<\nu} {\rm Re}\,(1 - U_{x\mu\nu})$, the gauge-fixing action $S_{\rm g.f.}(U)$, and the counterterm action $S_{\rm c.t.}(U)$. Altogether the action will depend on nine parameters: $g$, $\widetilde{\kappa}$, $\widetilde{r}$, $\kappa$, $\lambda_1, \ldots, \lambda_5$. As mentioned in the introduction, a ghost action is not needed [10]. We will refer to $S(U)$ as the action in the "vector picture," and $S(\phi_x^\dagger U_{\mu x} \phi_{x+\hat{\mu}})$ as the action in the "Higgs picture."

A naive lattice discretization of the continuum Lorentz gauge-fixing action leads to

$$S_{\rm g.f.}^{\rm naive}(U) = \widetilde{\kappa} \, \sum_x (\sum_\mu \Delta_\mu^- {\rm Im}\, U_{\mu x})^2 \, , \tag{4}$$

with $\widetilde{\kappa} = 1/(2g^2\xi)$ and $\Delta_\mu^- f_{\mu x} = f_{\mu x} - f_{\mu x-\hat{\mu}}$. The problem with this naive lattice discretization is that the classical vacuum of the action $S_{\rm G}(U) + S_{\rm g.f.}^{\rm naive}(U)$ is not unique [5]. It is easy to see that $S_{\rm G}(U) + S_{\rm g.f.}^{\rm naive}(U)$ has absolute minima for a dense set of lattice Gribov copies $U_{\mu x} = g_x^\dagger g_{x+\hat{\mu}}$ of $U_{\mu x} = 1$, for particular sets of $g_x$. An example of such a lattice Gribov copy is obtained for $g_x = -1$, $x = x_0$ and $g_x = +1$, $x \neq x_0$. These lattice Gribov copies are lattice artifacts with no counterpart in the continuum. A perturbative treatment of this naive lattice model is not feasible, since the expansion would have to be carried out coherently around the infinitely many classical vacua.

The unwanted lattice Gribov copies can be removed by adding a higher-dimensional operator to the naive gauge-fixing action of eq. (4). This procedure is similar to Wilson's idea of removing species doublers from the naive lattice fermion action. We adopt the following gauge-fixing action

$$S_{\rm g.f.}(U) = S_{\rm g.f.}^{\rm naive}(U) + \widetilde{r}\,\widetilde{\kappa} \, \sum_x \{A_x^2 - B_x^2\} \, , \tag{5}$$

with $A_x = \frac{1}{2}(C_x + C_x^\dagger)$, $C_x = \sum_y \Box_{xy}\,(U)$, $B_x = \frac{1}{4}\sum_\mu ({\rm Im}\, U_{\mu x-\hat{\mu}} + {\rm Im}\, U_{\mu x})^2$ and $\Box(U)_{xy} =$

$\sum_\mu \{U_{\mu x}\delta_{x+\hat{\mu},y} + U^\dagger_{\mu x-\hat{\mu}}\delta_{x-\hat{\mu},y} - 2\delta_{x,y}\}$. The new parameter $\widetilde{r}$ may be viewed as the analog of the Wilson parameter. (In previous work only the special case $\widetilde{r}=1$ was considered.) The new term in eq. (5) is irrelevant in the technical sense, yet one can show [6] that $S_{\rm g.f.}(U)$ has a unique absolute minimum at $U_{\mu x}=1$ for $\widetilde{r},\widetilde{\kappa}>0$. Perturbation theory in $1/\widetilde{\kappa}$ is in this case well-defined.

The counterterm action in eq. (3) is

$$S_{\rm c.t.}(U) = -2\kappa \sum_{\mu x} {\rm Re} U_{\mu x} - \lambda_1 \sum_{x\mu\nu} (\Delta^-_\nu \ {\rm Im} U_{\mu x})^2$$
$$-\lambda_2 \sum_{x\mu} (\Delta^-_\mu {\rm Im} U_{\mu x})^2 - \lambda_3 \sum_x (\sum_\mu \Delta^-_\mu {\rm Im} U_{\mu x})^2$$
$$-\lambda_4 \sum_x (\sum_\mu ({\rm Im} U_{\mu x})^2)^2 - \lambda_5 \sum_{x\mu} ({\rm Im} U_{\mu x})^4 \ . \qquad (6)$$

It contains the six relevant and marginal operators which are allowed by the exact lattice symmetries [4]. The coefficients $\kappa$, $\lambda_1,\ldots,\lambda_5$ are determined by the requirement that gauge invariance is restored in the continuum limit. The term proportional to $\kappa$ is a mass counterterm for the gauge field. It is the only dimension-two counterterm; all other counterterms are of dimension four. The terms proportional to $\lambda_1$, $\lambda_2$ and $\lambda_3$ are wave-function renormalization counterterms, and the terms proportional to $\lambda_4$ and $\lambda_5$ are needed to eliminate quartic photon self-interactions.

## 3. PHASE DIAGRAM

The traditional U(1) gauge-Higgs model (with a group-valued Higgs field) corresponds to the special case $\widetilde{\kappa}=0$, $\lambda_1,\ldots,\lambda_5=0$. The $(g,\kappa)$-phase diagram of this model is well known. At small $g$ it contains a Higgs and a Coulomb phase which are separated by a phase transition which is most likely of second order [13]. The spectrum in the Higgs phase contains a massive vector and a massive Higgs boson which scale when the phase transition is approached. The Higgs and Coulomb phases turn in the limit $g\to 0$ into paramagnetic (PM) and ferromagnetic (FM) phases, respectively. We will use the notation FM and PM also for the Higgs and Coulomb phases. At $g \gtrsim 1$ the phase diagram contains also a confinement phase which is analytically connected with the Higgs phase. This phase seems to be an artifact of the lattice regularization with compact fields. In the following we will take $g$ sufficiently smaller than 1 to avoid the confinement phase.

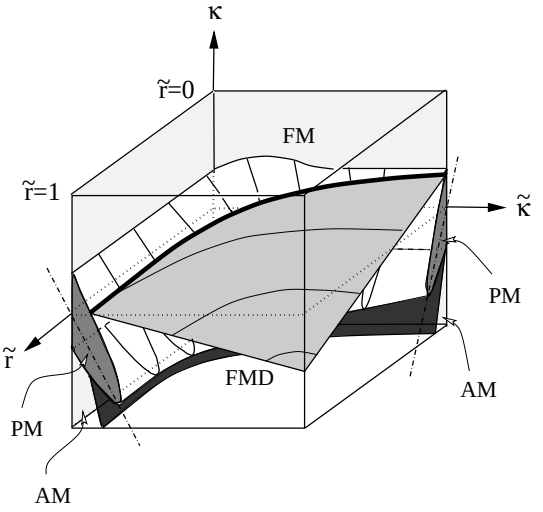


Figure 1. *Schematic three-dimensional plot of the $(\kappa,\widetilde{\kappa},\widetilde{r})$-phase diagram at $g=0.6$ for $0\le\widetilde{r}\le 1$. The dashed-dotted lines mark the intersection of the symmetry surface with two faces of the cube.*

The phase diagram is qualitatively different at large $\widetilde{\kappa}$, where rough gauge field configurations are strongly suppressed by the gauge-fixing action. In this region the phase diagram is controlled by the *classical potential*

$$V_{\rm cl}(A_\mu) = \kappa g^2 A^2 + \tfrac{1}{2}\, g^6\, \widetilde{\kappa}\, \widetilde{r}\, A^2\, A^4$$
$$-\lambda_4\, g^4\, (A^2)^2 - \lambda_5\, g^4\, A^4 \ + \cdots, \qquad (7)$$

where $A^k \equiv \sum_\mu A^k_\mu$. For each term in eq. (3) we have kept only the leading-order term in $g^2$ after substituting $U_{\mu x} = e^{igA_\mu}$ with $A_\mu$ constant. For $\widetilde{\kappa}\widetilde{r}>0$, $\lambda_4=\lambda_5=0$, minimization of the classical potential (7) gives $g\,A_\mu = 0$ for $\kappa\ge 0$ and $g\,A_\mu = \pm\,(|\kappa|/(6\,\widetilde{\kappa}\,\widetilde{r}))^{1/4}$ for $\kappa<0$ with $\mu=1,\ldots,4$. (See ref. [6] for $\lambda_4,\lambda_5\neq 0$.) Thus, classically, $\kappa=\kappa_{\rm FM-FMD}=0$ corresponds to a continuous phase transition between the FM phase where $\langle A_\mu\rangle = 0$ and the gauge boson is massive, and the FMD phase where $\langle A_\mu\rangle \neq 0$. In the FMD phase (hypercubic) rotation invariance

is broken spontaneously. *At* the phase transition one has both $\langle g\, A_\mu \rangle = 0$ and a massless photon.

We determined the three-dimensional $(\kappa, \widetilde{\kappa}, \widetilde{r})$-phase diagram at $g = 0.6$ by performing extensive Monte Carlo simulations and a mean-field analysis. The path integral (2) is invariant under the transformation $U_{\mu x} \to -U_{\mu x}$, $\phi_x \to \phi_x$, $\kappa \to -\kappa - 32\widetilde{\kappa}\,\widetilde{r}$, $\widetilde{\kappa} \to \widetilde{\kappa}$, $\widetilde{r} \to \widetilde{r}$, and we therefore restricted ourselves to the $\kappa \geq -16\,\widetilde{\kappa}\,\widetilde{r}$ region of the $(\kappa, \widetilde{\kappa}, \widetilde{r})$-phase diagram. Following ref. [14], the mean-field calculation was carried out in the Higgs picture. The saddle-point equations were solved numerically. The Monte Carlo simulations were mainly performed in the vector picture on a $4^4$ lattice. For more information about the technical details, see ref. [15].

A schematic plot of the $(\kappa, \widetilde{\kappa}, \widetilde{r})$-phase diagram which results from many scans at fixed $\widetilde{\kappa}$ or fixed $\widetilde{r}$ is displayed in fig. 1. The plot shows that, above the symmetry surface, the large-$\widetilde{\kappa}\widetilde{r}$ region is filled by FM or FMD phases (as prediced by the classical field approximation, cf. eq.(7)), whereas the small-$\widetilde{\kappa}\widetilde{r}$ region is filled by FM or PM phases. The large- and small-$\widetilde{\kappa}\widetilde{r}$ regions are separated by the FM-PM-FMD tricritical line (heavy line in fig. 1). In the region $\widetilde{r} < 0 < \widetilde{\kappa}$, which is not shown in fig. 1, there is another FM-PM-AM tricritical line. When increasing $\widetilde{\kappa} > 0$, this FM-PM-AM tricritical line and the FM-PM-FMD tricritical line (see fig. 2a) approach each other and finally meet at a quadricritical point which can be approached from any of the PM, FM, AM or FMD phases. Two scenarios are consistent with our Monte Carlo results. 1.) The PM phase extends to arbitrarily large $\widetilde{\kappa}$ and the quadricritical point is situated at $\widetilde{r} = \widetilde{r}_c$, $\widetilde{\kappa} = \infty$. 2.) The quadricritical point occurs at a finite $\widetilde{\kappa}$, beyond which one has a FM-AM-FMD tricritical line. In this case we have a FM-AM-FMD tricritical point at $\widetilde{r} = \widetilde{r}_c$, $\widetilde{\kappa} = \infty$. Our Monte Carlo data and the results from the mean-field analysis indicate that $\widetilde{r}_c$ is very close to zero.

Let's now consider the scaling region for the model defined by letting $g \ll 1$, while holding the gauge parameter $\xi$ fixed (and appropriately tuning the counterterms; recall that due to triviality there is strictly speaking no non-trivial continuum limit). This corresponds to a very large

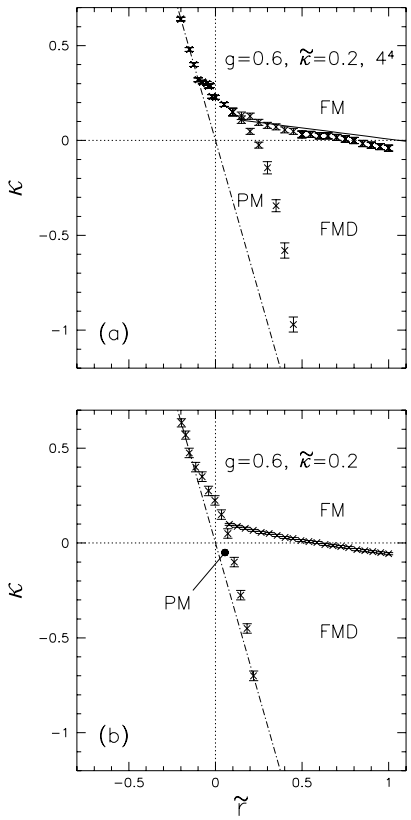


Figure 2. *Monte Carlo (fig. a) and mean-field (fig. b) $(\kappa, \widetilde{r})$-phase diagrams at $\widetilde{\kappa} = 0.2$ and $g = 0.6$. Results are shown only above the (dashed-dotted) symmetry line. Under the symmetry transformation (see text) FM is mapped into AM while PM and FMD are mapped onto themselves.*

value of $\widetilde{\kappa}$. For $\widetilde{r} > \widetilde{r}_c$ we have to approach the FM-FMD phase transition from the FM side to obtain a massless photon. (We will see in the next section that the spectrum contains no Higgs particle.) In the case of the naive gauge-fixing action (4) at $\widetilde{\kappa} \gg 1$, however, one is in the vicinity of a tri-or quadricritical point. It is therefore likely that the scaling region of the naive gauge-fixing action belongs to a universality class *different* from the FM-FMD transition at $\widetilde{r} > \widetilde{r}_c$ and large $\widetilde{\kappa}$. Finally for $\widetilde{r} < \widetilde{r}_c$ we hit for $\widetilde{\kappa} \to \infty$ a FM-AM phase transition when we lower $\kappa$ in the

FM phase. This transition is of first order and a continuum limit cannot be performed.

As an example of our phase-diagram scans we display in fig. 2 the $(\kappa, \widetilde{r})$-phase diagrams at $\widetilde{\kappa} = 0.2$. Fig. 2a was obtained by Monte Carlo simulations and fig. 2b by the mean-field analysis. The two plots show that there are two tricritical points: a FM-PM-FMD tricritical point at $\widetilde{r} > 0$ and a FM-PM-AM tricritical point at $\widetilde{r} < 0$. The first-order FM-AM phase transition is located on the symmetry line (dashed-dotted line). As mentioned above, to tree level order $\kappa_{\mathrm{FM-FMD}} = 0$. Fig. 2a shows that the data for the FM-FMD phase transition deviate from that value. We have therefore calculated $\kappa_{\mathrm{FM-FMD}}$ (and also $\lambda_1$, $\lambda_2$ and $\lambda_3$) to one-loop order in perturbation theory. The result for $\kappa_{\mathrm{FM-FMD}}$ is represented in fig. 2a by the solid line which is in better agreement with the numerical data.

The Monte Carlo simulations and the mean-field analysis lead to a similar picture, except at $\widetilde{r} \sim 0$, $\widetilde{\kappa} \gtrsim 0.25$. There the mean-field analysis predicts a FMD phase while the Monte Carlo data strongly favors a PM phase. In both cases, the transition to the FM phase appears to be first order. (It is known that mean-field analysis tends to prefer ordered over disordered phases. Of course we cannot rule out that at yet larger $\widetilde{\kappa}$ PM is replaced by FMD.) For more details see ref. [15].

## 4. SPECTRUM

At the FM-FMD phase transition, the action (3) should provide a new lattice discretization of a theory of free photons. Unlike in the FM phase of the U(1) gauge-Higgs model (mentioned in the beginning of Sec. 3) no Higgs particle should exist. We have analyzed the spectrum by computing the vector and Higgs two-point functions defined respectively as

$$\Delta^V_{\mu\nu}(p) = \frac{1}{L^3\,T}\langle \sum_{x,y} \mathrm{Im}U_{\mu x}\ \mathrm{Im}U_{\nu y}\ e^{ip(x-y)}\rangle\ , \quad (8)$$

$$\Delta^H_{\mu\nu}(p) = \frac{1}{L^3\,T}\langle \sum_{x,y} \mathrm{Re}U_{\mu x}\ \mathrm{Re}U_{\nu y}\ e^{ip(x-y)}\rangle\ , \quad (9)$$

near the FM-FMD transition, both in perturbation theory and numerically.

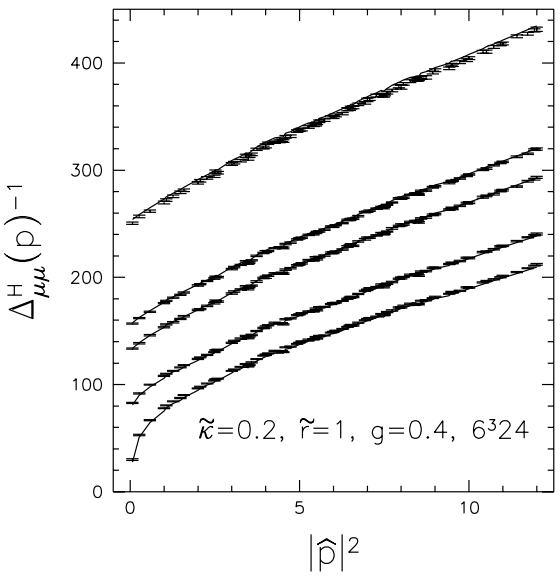


Figure 3. $\Delta^H_{\mu\mu}(p)^{-1}$ *as a function of* $|\widehat{p}|^2$. *The error bars represent the Monte Carlo data and the solid lines the perturbative results.*

The one-loop calculation of the vector propagator [15] shows that a free massless photon is obtained if the counterterm coefficients $\kappa$, $\lambda_1$, $\lambda_2$, and $\lambda_3$ are adjusted appropriately. The one-loop result for the vector propagator is in good agreement with the numerical data, which confirms that the spectrum at the FM-FMD phase transition indeed contains a free massless photon.

Next, we consider the Higgs two-point function. To leading order in perturbation theory $\Delta^H_{\mu\nu}(p) = \frac{1}{2}g^4 e^{i\,(p_\mu - p_\nu)/2} \sum_k \Delta^{V,(0)}_{\mu\nu}(k)\Delta^{V,(0)}_{\mu\nu}(p+k)$ where $\Delta^{V,(0)}_{\mu\nu}(p) = [(m^2+\widehat{p}^2)\delta_{\mu\nu} - (1-1/\xi)\ \widehat{p}_\mu\ \widehat{p}_\nu]^{-1}$ is the tree-level vector propagator where $\widehat{p}_\mu = 2\sin(p_\mu/2)$ and $m = (2\ \kappa\ g^2)^{1/2}$ is the photon mass. It is evident that $\Delta^H_{\mu\nu}(p)$ has a logarithmic cut rather than an isolated pole, in the limit $\kappa \to 0$. It could however happen that the existence of a Higgs boson is due to non-perturbative effects, and it is therefore important to compare the above perturbative formula for $\Delta^H_{\mu\nu}(p)$ with Monte Carlo data. To this end, we have determined the Higgs two-point function in eq. (9) for

$\mu = \nu$ and $p_\mu = 0$ numerically at a series of points in the FM phase in the vicinity of the FM-FMD phase transition. The simulations were performed on a $6^3 \times 24$ lattice and we set $g = 0.4$, $\widetilde{\kappa} = 0.2$, $\widetilde{r} = 1$, $\lambda_1 = \ldots = \lambda_5 = 0$. In fig. 3 we have plotted $\Delta^H_{\mu\mu}(p)^{-1}$ as a function of $|\widehat{p}|^2$. The five data sets from the top to bottom correspond to $\kappa = 0.8$, 0.4, 0.3, 0.1 and 0.01. The FM-FMD phase transition is situated at $\kappa \approx 0$.

If the Higgs propagator had an isolated pole, the data should fall on a straight line at small momenta. A glance at fig. 3 shows that this is not the case for the smaller $\kappa$ values. The data exhibit a clear cusp at small momenta which is getting more pronounced when the FM-FMD transition is approached, and which is due to the logarithmic singularity. The solid lines in fig. 3 were obtained by evaluating the above perturbative expression for $\Delta^H_{\mu\nu}(p)$ on a lattice of the same size and for the same parameter values which were used in the simulations. The good agreement of the perturbative result with the Monte Carlo data gives strong evidence that a Higgs particle does not exist at the FM-FMD phase transition.

If a Higgs particle is indeed absent, one expects the coordinate-space correlation function $G^H_{\mu\nu}(|x-y|) = \langle \mathrm{Re}U_{\mu x}\ \mathrm{Re}U_{\nu y}\rangle - \langle \mathrm{Re}U_{\mu x}\rangle\langle \mathrm{Re}U_{\nu x}\rangle$ to factorize at large separation $|x-y| \to \infty$ as $G^H_{\mu\nu}(|x-y|) = C_{\mu\nu}\ [G^V_{\mu\nu}(|x-y|)]^2$, where $G^V_{\mu\nu}(|x-y|) = \langle \mathrm{Im}U_{\mu x}\ \mathrm{Im}U_{\nu y}\rangle$ is the vector correlation function and $C_{\mu\nu}$ is a constant which can be determined in perturbation theory. It is easy to see that to leading order $C_{\mu\nu} = 1/2$. In ref. [15] we show explicitly that factorization holds also at the next-to-leading order. In our Monte Carlo simulations, we have computed $G^H_{\mu\nu}(|x-y|)$ and $G^V_{\mu\nu}(|x-y|)$. We find that the ratio $R = G^H_{\mu\nu}(|x-y|)/G^V_{\mu\nu}(|x-y|)^2$ approaches indeed a constant at large separations $|x-y|$ and that the data for this ratio are in excellent agreement with the perturbative results. These results confirm the absence of a Higgs particle.

## 5. OUTLOOK

As a next step the gauge-fixing approach should be generalized to non-abelian gauge theories which, even without fermions, is a difficult task. A naive discretization of the ghost sector is problematic due to the existence of (continuum) Gribov copies [16]. Among other problems, some copies will give rise to a negative sign of the Fadeev–Popov determinant [16], which may make numerical computations intractable. A way out may be to adopt the gauge-fixing procedure of ref. [17], in which the integrand in the path integral is guaranteed to be positive. This is presently under investigation.

WB and KCL thank the Institute of Physics of the University Siegen for support. MG is supported in part by the US Dept. of Energy. YS is supported in part by the Israel Science Foundation.

## REFERENCES

1. Y. Shamir, Nucl. Phys. B (Proc. Suppl.) 47 (1996) 212
2. M. Lüscher, Nucl. Phys. B549 (1999) 295
3. M. Lüscher, hep-lat/9904009
4. A. Borelli, L. Maiani, G.-C. Rossi, R. Sisto, M. Testa, Nucl. Phys. B333 (1990) 335
5. Y. Shamir, Phys. Rev. D57 (1998) 132
6. M.F.L. Golterman, Y. Shamir, Phys. Lett. B399 (1997) 148
7. W. Bock, M.F.L. Golterman, Y. Shamir, Phys. Rev. D58 (1998) 054506
8. W. Bock, M.F.L. Golterman, Y. Shamir, Phys. Rev. D58 (1998) 034501
9. W. Bock, M.F.L. Golterman, Y. Shamir, Phys. Rev. Lett. 80 (1998) 3444
10. W. Bock, M.F.L. Golterman, Y. Shamir, Phys.Rev. D58 (1998) 097504
11. S. Basak, A.K. De, these proceedings
12. Y. Shamir, Phys. Rev. Lett. 71 (1993) 2691; hep-lat/9307002
13. V. Azcoiti, G. di Carlo, A.F. Grillo, Phys. Lett. B258 (1991) 207
14. J.-M. Drouffe, J.-B. Zuber, Phys. Rept. 102 (1983) 1
15. W. Bock, M.F.L. Golterman, K.C. Leung, Y. Shamir, in preparation
16. V. Gribov, Nucl. Phys. B139 (1978) 1
17. C. Parrinello, G. Jona-Lasinio, Phys. Lett. B251 (1990) 175; D. Zwanziger, Nucl. Phys. B192 (1981) 259